HHS Public Access

Author manuscript

*Cell*. Author manuscript; available in PMC 2017 June 16.

Published in final edited form as:

*Cell*. 2016 June 16; 165(7): 1621–1631. doi:10.1016/j.cell.2016.05.024.

# Engineered Bispecific Antibodies with Exquisite HIV-1-Neutralizing Activity

**Yaoxing Huang**[1,3], **Jian Yu**[1,3], **Anastasia Lanzi**[1,3], **Xin Yao**[1], **Chasity D. Andrews**[1], **Lily Tsai**[1], **Mili R. Gajjar**[1], **Ming Sun**[1], **Michael S. Seaman**[2], **Neal N. Padte**[1], and **David D. Ho**[1]

[1]Aaron Diamond AIDS Research Center, The Rockefeller University; 455 First Avenue; New York, NY 10016; USA.

[2]Beth Israel Deaconess Medical Center, Harvard Medical School, Boston, MA 02215; USA.

## SUMMARY

While the search for an efficacious HIV-1 vaccine remains elusive, emergence of a new generation of virus-neutralizing monoclonal antibodies (mAbs) has re-ignited the field of passive immunization for HIV-1 prevention. However, the plasticity of HIV-1 demands additional improvements to these mAbs to better ensure their clinical utility. Here, we report engineered bispecific antibodies that are the most potent and broad HIV-neutralizing antibodies to date. One bispecific antibody, $10E8_{V2.0}$/iMab, neutralized 118 HIV-1 pseudotyped viruses tested with a mean 50% inhibitory concentration ($IC_{50}$) of 0.002 μg/mL. $10E8_{V2.0}$/iMab also potently neutralized 99% of viruses in a second panel of 200 HIV-1 isolates belonging to clade C, the dominant subtype accounting for ~50% of new infections worldwide. Importantly, $10E8_{V2.0}$/iMab reduced virus load substantially in HIV-1-infected humanized mice, and also provided complete protection when administered prior to virus challenge. These bispecific antibodies hold promise as novel prophylactic and/or therapeutic agents in the fight against HIV-1.

## Graphical Abstract

**Contact Information:** David D. Ho (dho@adarc.org).

[3]Co-first author



**AUTHOR CONTRIBUTIONS**

Y.H., J.Y., X.Y. and M.S. identified and generated all of the HIV CrossMAbs and variants and characterized their in vitro activity and in vivo pharmacokinetics. A.L., L.T. and M.R.G. conducted the HIV treatment and prevention studies in humanized mice, and A.L drafted the humanized mouse studies section of the manuscript. C.D.A. conducted the SEC experiments. M.S.S. conducted the in vitro neutralization studies against the 118 multi-clade and 200 clade-C HIV envelope pseudotyped virus panels. Y.H., N.N.P. and D.D.H. wrote the overall manuscript and were responsible for project management and supervision. All authors contributed to the design of experiments and analyses of experimental data.

**ACCESSION NUMBERS**

Nucleotide sequences for heavy-chain and light-chain variable regions of 10E8 mAb or CrossMAb variants generated have been deposited under GenBank accession numbers KX077232 through KX077241.

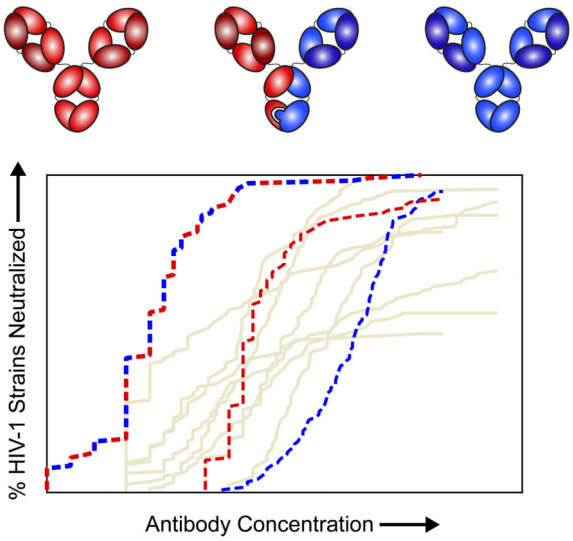


## INTRODUCTION

The field of HIV-1 neutralizing antibodies has progressed rapidly in recent years (Mascola and Haynes, 2013). Numerous potent and broad neutralizing mAbs have been isolated from infected humans since 2009 (Blattner et al., 2014; Doria-Rose et al., 2014; Huang et al., 2012; Mouquet et al., 2012a; Rudicell et al., 2014; Scheid et al., 2011; Sok et al., 2014; Walker et al., 2011; Walker et al., 2009; Wu et al., 2010). Impressive anti-HIV-1 activity has been noted with select mAb combinations in vitro (Klein et al., 2012; Kong et al., 2015; Sok et al., 2014) and in vivo (Halper-Stromberg et al., 2014; Klein et al., 2012). Structure-based modifications of antibodies have also resulted in further improvements in anti-HIV-1 activity (Diskin et al., 2011). We (Pace et al., 2013b; Sun et al., 2014) and others (Gardner et al., 2015) have engineered antibodies with dual specificity that showed marked enhancement of virus-neutralization breadth and potency. It should be noted, however, that the aforementioned anti-HIV-1 bispecific antibodies or antibody-like molecules deviate from the normal antibody structure, thereby raising concerns about their potential immunogenicity, unfavorable pharmacokinetic properties, and manufacturing challenges. One approach to construct bispecific antibodies with normal architecture utilizes the so-called CrossMAb technology (Schaefer et al., 2011). In this study, we used this technology to generate a library of bispecific antibodies, which were then characterized for their activities against HIV-1. Two bispecific antibodies, $10E8_{V2.0}$/iMab and $10E8_{V1.1}$/P140, emerged that potently neutralized the majority of circulating HIV-1 strains tested in vitro. $10E8_{V2.0}$/iMab was advanced into proof-of-concept in vivo studies, demonstrating potent activity as a single agent in humanized mouse models of HIV-1 treatment and prevention.

## RESULTS

### HIV CrossMAbs possess potent and broad antiviral activity against HIV-1

As schematically shown in Fig. 1A, the creation of a “knob” in one H-chain and a “hole” in the other H-chain favors the formation of H-chain heterodimers, while the “crossover” of CL

and CH1 sequences in one arm of the antibody favors correct H-L-chain pairings in both arms. Each bispecific antibody was engineered, as shown in Fig. 1A, so that one arm targeted either the human CD4 receptor via the Fab of ibalizumab (iMab) (Burkly et al., 1992; Jacobson et al., 2009; Pace et al., 2013a; Reimann et al., 1997; Song et al., 2010; Toma et al., 2011) or the human CCR5 co-receptor via the Fab of mAb PRO140 (P140) (Tenorio, 2011; Trkola et al., 2001). The other arm targeted one of the five neutralizing epitope clusters on the viral envelope glycoproteins using one of the recently isolated HIV-1-neutralizing mAbs (Blattner et al., 2014; Huang et al., 2012; Scheid et al., 2011; Walker et al., 2011). In this fashion, we created a library of 20 bispecific antibodies, including the specific examples in Fig. 1A.

To confirm the dual specificity of the HIV CrossMAb format, we characterized the binding activity of 3BNC117/iMab, for example, by surface plasmon resonance and ELISA. This bispecific CrossMAb bound both soluble human CD4 and HIV-1 gp120 monomer with affinities that are similar to those of the parental antibodies (Fig. S1A and data not shown). Moreover, 3BNC117/iMab successively bound soluble human CD4 and monomeric gp120 (Fig. S1B), again confirming its dual specificity.

Each bispecific antibody in the library, along with its parental mAbs, was then tested for HIV-1 neutralization in vitro against a panel of 118 HIV-1 pseudotyped viruses representing diverse clades and geographic origins (Seaman et al., 2010). Most of the bispecific antibodies were not evidently better in neutralizing HIV-1 than their parental mAbs. As examples, $IC_{50}$ and maximum percent inhibition (MPI) results for PGT145/iMab, PGT145/P140, 3BNC117/iMab, 3BNC117/P140, PGT128/iMab, PGT128/P140, PGT151/iMab, and PGT151/P140 are shown in Fig. 1B. Likewise, $IC_{80}$ results are displayed in a different format in Figs. S2A to S2D. Two bispecific antibodies stood out, however, in their virus-neutralizing activity. 10E8/P140 and 10E8/iMab were found to have mean $IC_{50}$ of 0.001 μg/mL and 0.002 μg/mL, respectively, as well as neutralization breadth (as assessed by >50% neutralization) of 99% and 100%, respectively (Fig. 1B). Both the mean $IC_{50}$ and maximum percent inhibition (MPI) for 10E8/P140 and 10E8/iMab were each significantly different from the mean $IC_{50}$ and MPI of parental mAbs 10E8, P140, and iMab ($P < 0.0003$ for all pairs). The gain in HIV-1 neutralization activity was even more discernible when comparing $IC_{80}$ of these two bispecific antibodies to those of their parental mAbs (Fig. S2E). Only three viruses in this HIV-1 panel were relatively resistant to neutralization by 10E8/P140 and 10E8/iMab. Analysis of envelope sequences for these three viral strains (WEAU_d15_410_5017 in clade B, X2088_c9 in clade G and 3103.v3.c10 in clade ACD) showed, as expected, substantial deviations from the known 10E8 epitope sequence (Huang et al., 2012) in the membrane proximal external region (MPER) of gp41 (data not shown).

The remarkable HIV-1 neutralization profiles of 10E8/P140 and 10E8/iMab were readily apparent when presented on an antiviral coverage plot (Fig. 1C), comparing favorably with the antiviral coverage of penta-mix, a mixture of five distinct potent HIV-1-neutralizing mAbs (Klein et al., 2012). Moreover, both 10E8/P140 and 10E8/iMab exhibited HIV-1 neutralization potencies that were orders of magnitude greater than their parental mAbs (Fig. 1C).

## Neutralization studies to elucidate the mechanism of action of a potent HIV CrossMAb

To better understand how the linkage of a host-cell-targeting antibody to a virus-envelope-targeting antibody could mediate such a marked enhancement in antiviral activity, we conducted a series of experiments using 10E8/P140, the antiviral potency of which was hundreds of fold greater than those of its parental mAbs (Fig. 1C). We first asked whether the enhancement in potency was due to P140 and 10E8 acting together synergistically or whether the physical linkage of P140 and 10E8 in a single antibody molecule was required. As shown in the example in Fig. 2A, a 1:1 mixture of P140 and 10E8 mAbs neutralized HIV-1 only as effectively as the more potent of the two parental mAbs, but no better. In contrast, 10E8/P140 neutralized the virus more efficiently, indicating that the physical linkage of the 10E8 and P140 moieties is important in the enhancement of potency.

We next asked what the relative contribution of each antibody arm was to the potency of 10E8/P140. To evaluate the P140 arm, we substituted it with one of a number of other host-cell-binding mAbs or with a non-membrane-binding antibody control, while keeping the 10E8 arm constant. HIV-1 neutralization was weakest when 10E8 was linked to X19, the non-membrane-binding control antibody, followed by linkage to 4D5 or 515H7, which targeted HER2 or CXCR4, respectively, on the host cell membrane (Fig. 2B). The most potent virus neutralization was observed with linkage to iMab or P140, which targeted cell surface CD4 or CCR5, respectively. These findings suggest that the location on the host cell membrane to which 10E8 is targeted is crucial to the potency enhancement of these bispecific antibodies.

We then assessed the importance of the 10E8 arm of 10E8/P140 by substituting it with another MPER-targeting mAb that is known to be less potent, 4E10 (Stiegler et al., 2001), or with a 10E8 mutant containing a single point mutation that attenuated its binding to MPER, Δ10E8. In the representative results shown in Fig. 2C, all three of these MPER-binding bispecific antibodies were capable of neutralizing HIV-1; however, 10E8/P140 was the most potent. This finding suggests that the binding affinity of the 10E8 arm does contribute to the overall potency of the bispecific antibody. Interestingly, although Δ10E8 and 4E10 had little or no virus neutralizing activity on their own at the concentrations tested, substantial activity was observed for Δ10E8/P140 and 4E10/P140 (Fig. 2C), demonstrating once again the importance of specific targeting. Taken together, the findings from this series of experiments suggest that the potency of 10E8/P140 is likely the outcome of concentrating 10E8 at the right location on the cell surface, perhaps precisely at the site of viral entry. We reached a similar conclusion previously after studying other anti-HIV-1 bispecific antibodies with a different architecture (Pace et al., 2013b).

## 10E8 mAb and 10E8-containing CrossMAbs exhibit physicochemical heterogeneity

Encouraged by their potent and broad antiviral activity, we initiated developability and manufacturability studies on both 10E8/P140 and 10E8/iMab to evaluate their potential as clinical candidates for HIV-1 prevention and/or treatment. Size exclusion chromatography (SEC) was used to assess the purity of these bispecific antibody preparations, and we observed physicochemical heterogeneity in both 10E8/P140 and 10E8/iMab, as evidenced by double peaks in their chromatographs (Fig. 3A). The double peaks, however, could not be

explained by antibody aggregation, since such aggregates would be detected at ~7.7 mL with the SEC conditions utilized. To investigate the underlying cause of the physicochemical heterogeneity, we analyzed another CrossMAb, 3BNC117/iMab, by SEC and observed a single homogenous peak, suggesting that the heterogeneity was not necessarily the outcome of the CrossMAb technology. We therefore conducted SEC analysis on the parental antibodies of 10E8/P140 and 10E8/iMab: iMab, P140 and 10E8. As expected for mAbs already in clinical development, both iMab and P140 exhibited a single homogenous peak, although these antibodies, with comparable molecular weights, interacted differently with the column resulting in differences in their elution profiles (Fig. 3B). In contrast, 10E8 exhibited double peaks similar to those observed for 10E8/P140 and 10E8/iMab. These findings suggested that the 10E8 arm in both 10E8/P140 and 10E8/iMab was responsible for the physicochemical heterogeneity. This conclusion was confirmed when 4E10 was substituted for 10E8 in the bispecific antibody to yield 4E10/P140, which was found to be homogeneous by SEC (Fig. 3A).

## Engineering HIV CrossMAb variants with improved developability, activity and manufacturability potential

The double peaks observed by SEC for 10E8, 10E8/P140, and 10E8/iMab could reflect molecular species with either different masses or different column-interacting properties. To discriminate between these possibilities, native mass spectroscopy (Rosati et al., 2014) was performed on deglycosylated preparations of 10E8 and 10E8/P140, revealing in each a single dominant molecular species of 146,823.1 ± 0.4 Da and 146,723.2 ± 0.6 Da, respectively (data not shown). There was no evidence of a major degradation product. Also, collecting fractions of 10E8/iMab after SEC and then re-analyzing these isolated 10E8/iMab fractions by SEC again revealed that the separated fractions once again displayed physicochemical heterogeneity (data not shown). These collective results raised the specter that preparations of 10E8 and 10E8-based bispecific antibodies contained “isoforms” that interacted with the SEC column differently.

It is known in the mAb field that antibodies can adopt more than one conformation (Liu et al., 2008). Importantly, antibodies with physicochemical heterogeneity have typically faced difficulties in clinical development, including poor pharmacokinetic properties (Goetze et al., 2010). We therefore attempted to solve this problem by conducting a series of experiments to examine the effect of antibody production and formulation conditions. These experiments included producing the antibody in the presence of reagents such as EDTA, acetic acid, L-lysine and copper (II) sulfate, which have been reported to improve the quality and yield of antibody production through the sequestration of metal ions, thereby decreasing potential enzymatic activity, or through the prevention of antibody disulfide bond reduction (Hutterer et al., 2013; Koterba et al., 2012; Mullan et al., 2011). Also included was an assessment of a histidine buffer-based formulation at pH 6.0, which has the potential to improve the stability of antibodies at the predicted isoelectric points of these bispecific antibodies as compared to similar antibodies in a phosphate buffered saline solution at pH 7.4 (Haverick et al., 2014; Lowe et al., 2011; Salinas et al., 2010). These combined efforts, however, failed to fix the physicochemical heterogeneity observed for 10E8/P140 and 10E8/iMab (data not shown). We then turned our attention to the reported somatic and germline

variants of 10E8 (Georgiev et al., 2014; Zhu et al., 2013) with the goal of finding variants with better physicochemical properties while retaining their anti-HIV-1 activity. After empirically testing 18 somatic and germline variants of 10E8, one variant, $10E8_{V1.0}$ (also known as H6L10 (Zhu et al., 2013)), was identified that exhibited a single homogeneous peak by SEC when produced as a mAb or as a bispecific antibody paired with P140 (Fig. 3C). Interestingly, the SEC profile of $10E8_{V1.0}$ paired with iMab continued to show double peaks, revealing the complex, context-dependent nature of physicochemical interactions mediated by certain residues in 10E8 or its variants. $10E8_{V1.0}$/P140 was tested for its anti-HIV-1 activity against the panel of 118 pseudotyped viruses, showing a 23-fold decrease in potency as compared to 10E8/P140 (Fig. 3D). $10E8_{V1.0}$/iMab showed a more modest 5-fold decrease in potency as compared to 10E8/iMab, but its physicochemical heterogeneity precluded its advancement.

We next created chimeras of 10E8 and $10E8_{V1.0}$, generated point mutations within these chimeras, and grafted the CDR regions of other MPER-binding mAbs into these chimeric mutants, in order to find new variants that would restore anti-HIV-1 activity and retain physicochemical homogeneity. Empirically, 38 variants were constructed and paired with P140 or iMab (Table S1), and each new bispecific antibody was tested for virus neutralization and physicochemical homogeneity. While most did not meet the desired profile, two new bispecific antibodies showed promise. $10E8_{V1.1}$/P140 and $10E8_{V2.0}$/iMab demonstrated physicochemical homogeneity (Fig. 4A) as well as impressive antiviral activity (Fig. 4B). Interestingly, the best 10E8 chimeric variant was different depending on whether it was paired with P140 or iMab, highlighting again the context-dependent nature of the physicochemical properties of these bispecific antibodies. $10E8_{V1.1}$/P140 was ~8-fold more potent than its predecessor, $10E8_{V1.0}$/P140, but was still ~3-fold less potent than the original 10E8/P140. $10E8_{V2.0}$/iMab, on the other hand, gained potency over the original 10E8/iMab (Fig. 4B). To further investigate their antiviral activities, we tested $10E8_{V1.1}$/P140 and $10E8_{V2.0}$/iMab in virus-neutralization assays against a panel of 200 viruses belonging to HIV-1 clade C (manuscript in preparation), the dominant subtype spreading throughout the world today. The virus-neutralizing potency and breadth observed for both bispecific antibodies remained significant (Fig. 4C). While $10E8_{V1.1}$/P140 was slightly less active against clade C viruses, $10E8_{V2.0}$/iMab retained a similar potency against viruses of this subtype.

Interestingly, we also observed that the physicochemical heterogeneity of 10E8/iMab and 10E8/P140 was associated with poor antibody bioavailability when administered to mice (Fig. 4D). The engineered HIV CrossMAb variants $10E8_{V2.0}$/iMab and $10E8_{V1.1}$/P140, which demonstrated physicochemical homogeneity by SEC, exhibited a ~2-fold increase in bioavailability in mice as compared to their non-engineered counterparts, 10E8/iMab and 10E8/P140. Thus, in addition to improved physicochemical homogeneity and satisfactory or improved HIV-1-neutralizing activity in vitro, the engineered variants $10E8_{V2.0}$/iMab and $10E8_{V1.1}$/P140 resulted in increased serum concentrations after administration in vivo.

### HIV CrossMAb 10E8$_{V2.0}$/iMab exhibits therapeutic efficacy in vivo

To ascertain its antiviral activity in vivo, we tested 10E8$_{V2.0}$/iMab in a humanized mouse model of HIV-1 infection (Berges and Rowan, 2011). Immunodeficient NSG mice (NOD.Cg-*Prkdc*$^{scid}$ *Il2rg*$^{tm1Wjl}$/SzJ) were reconstituted with human hematopoietic stem cells, as evidenced by the detection of human CD4 and CD8 T cells in blood. In the first series of experiments, the humanized mice were infected with the tier 2 clade B HIV-1$_{JR-CSF}$; the sensitivity of which to 10E8$_{V2.0}$/iMab and the parental antibodies was first assessed in vitro (Fig. S3). Once infection was documented for ≥ 4 weeks, the mice were divided into four groups and treated with weekly intraperitoneal administrations of 10E8$_{V2.0}$/iMab (0.5 mg), or with placebo (PBS), iMab (0.5 mg), or 1:1 mixture of iMab (0.25 mg) + 10E8$_{V2.0}$ (0.25 mg) as comparators. A weekly antibody dose of 0.5 mg was chosen to compare the efficacy of 10E8$_{V2.0}$/iMab to that of other antibodies used in previous treatment studies in the humanized mouse model (Klein et al., 2012; Luo et al., 2010), and blood was drawn from mice before each weekly antibody administration to confirm that detectable trough levels of antibody were present in vivo throughout the experiment (Fig. S4). While no to modest viral load reductions were observed in the comparator groups, mice receiving 10E8$_{V2.0}$/iMab demonstrated a significantly greater viral load reduction (Figs. 5A and 5B). The mean reduction of ~1.7 log at week 2 is not dissimilar to the degree of virus suppression reported for humanized mice treated with a penta-mix of potent neutralizing mAbs given at a dose of 4.5 mg weekly (Klein et al., 2012). After the initial virus suppression, HIV-1 rebounded in all but two of the 10E8$_{V2.0}$/iMab-treated mice. Sequencing of the rebounding viruses in iMab-treated or iMab+10E8$_{V2.0}$-treated mice showed evidence of Env mutations known to confer iMab resistance (Pace et al., 2013a; Toma et al., 2011) (Figs. 5C and S5), indicating that the observed antiviral pressure, at the doses given, was primarily exerted by iMab. In contrast, the viral rebound in mice treated with 10E8$_{V2.0}$/iMab was principally associated with mutations within the known 10E8 epitope in gp41 MPER (Huang et al., 2012) (Figs. 5C and S5). When a selection of these mutations (W672G, W672L, F673L) were each introduced into a molecular clone of HIV-1$_{JR-CSF}$, the resultant viruses were indeed substantially resistant to 10E8$_{V2.0}$ and 10E8$_{V2.0}$/iMab (Fig. 5D). Alternatively, the mutations found in the C3 or V5 regions (N339D, S463N), once introduced in the JR-CSF backbone, gave resistance to iMab, and a non-relevant mutation (G410R) did not give any resistance to any of the antibodies. These findings showed that the antiviral activity of 10E8$_{V2.0}$/iMab was mainly mediated by the 10E8$_{V2.0}$ arm.

### HIV CrossMAb 10E8$_{V2.0}$/iMab protects humanized mice against repeated systemic HIV-1 challenges

In the second series of in vivo experiments, we examined whether 10E8$_{V2.0}$/iMab could be used as pre-exposure prophylaxis (PrEP) against HIV-1 infection. Humanized mice were given PBS (controls) or 10E8$_{V2.0}$/iMab intraperitoneally at a dose (0.2 mg) known to completely coat CD4 receptors on circulating human T cells in the mice for at least seven days (Fig. S6). One day later, all mice were challenged with HIV-1$_{JR-CSF}$ (200,000 TCID$_{50}$) intraperitoneally, and the same dose of 10E8$_{V2.0}$/iMab was given weekly for another 8 weeks to the treated group. By two weeks post virus challenge, 3 of 19 control mice remained aviremic, whereas 7 of 7 treated mice showed no evidence of infection when followed to week 4 (Fig. 6A). Two more virus challenges were therefore given (200,000

$TCID_{50}$ on week 4 and 250,000 $TCID_{50}$ on week 6) to the $10E8_{V2.0}$/iMab-treated mice, but these animals remained aviremic for the duration of the experiment (Fig. 6A), even long after the bispecific antibody was no longer detectable (Fig. 6B). The above findings strengthen the notion that $10E8_{V2.0}$/iMab is a potent HIV-1-neutralizing agent with potential clinical utility.

## DISCUSSION

In summary, we have engineered two architecturally normal bispecific antibodies, $10E8_{V1.1}$/P140 and $10E8_{V2.0}$/iMab, with exquisite potency and breadth in neutralizing multiple clades of HIV-1. About 98% of the viruses tested were neutralized by each antibody (Fig. 4C), with a geometric mean $IC_{50}$ of ~0.002 μg/mL (Table S2). In terms of in vitro neutralization against a large panel of diverse HIV-1 strains, both $10E8_{V1.1}$/P140 and $10E8_{V2.0}$/iMab compared quite favorably against other anti-HIV-1 antibodies in clinical development, as shown in Fig. 7, including select Env-directed mAbs (Doria-Rose et al., 2014; Mouquet et al., 2012a; Rudicell et al., 2014; Scheid et al., 2011; Sok et al., 2014; Walker et al., 2011; Wu et al., 2010), an antibody-like construct with dual specificities (Gardner et al., 2015), and two- or four-antibody mixtures (Kong et al., 2015; Sok et al., 2014). In short, both bispecific antibodies appear to be the broadest and most potent HIV-1-neutralizing biologic agents described to date.

Moreover, $10E8_{V2.0}$/iMab has been shown to be active in both treating and preventing HIV-1 in a humanized mouse model (Figs. 5 and 6). Our treatment study demonstrated that using a low dose of 0.5 mg per week of $10E8_{V2.0}$/iMab in humanized mice could lead to a substantial reduction of 1.7 log in viral load two weeks after beginning treatment. Using a mAb as monotherapy, leading to a transient decline in plasma viremia, has been described previously in humanized mice using a range of different Abs (Klein et al., Nature 2012), as was observed in rhesus macaques treated with 3BNC117 Ab (Barouch et al., Nature 2013). These findings suggest that an antibody combination therapy would be needed for sustained viral suppression. Two recent clinical trials using VRC01 and 3BNC117 monotherapy also demonstrated only transient decline in viremia in HIV-infected participants (Caskey et al., Nature 2015; Lynch et al., Sci Transl Med. 2015). Likewise, our results demonstrated that infusions of the bispecific $10E8_{V2.0}$/iMab lead to a transient viral reduction. However, the peak viral reduction we have observed is greater than previously described for single mAbs or combination of three mAbs (Klein et al., Nature 2012). Moreover, it should be noted that two $10E8_{V2.0}$/iMab-treated mice had viral load reductions of nearly 2 logs without any evidence of a viral rebound (Fig. 5A). We showed that the antiviral activity of $10E8_{V2.0}$/iMab was mainly mediated by the $10E8_{V2.0}$ arm (Figs. 5C and D), which is consistent with an earlier conclusion that the exquisite potency of our bispecific antibody is due to concentrating 10E8 on the cell membrane at the site of viral entry (Fig. 2B). By anchoring 10E8 at the right place on the cell surface, we have transformed a broad and weak HIV-neutralizing mAb into a broad and potent one.

Regarding the use of $10E8_{V2.0}$/iMab in a prevention setting, our results are unprecedented in that all mice were protected from repeated systemic challenges with a relatively low dose of antibody injection. The only complete protection against systemic challenge in a humanized

mouse model reported to date was achieved against the tier 1 X4 virus, NL4.3 (Balazs et al., 2012; Gardner et al., 2015), whereas passive administration of $10E8_{V2.0}$/iMab could protect mice against the tier 2 R5 virus, JR-CSF. Using a vectored immunoprophylaxis system where a HIV antibody was continuously expressed at plasma concentrations greater than 100 μg/mL did not protect all mice against one systemic JR-CSF challenge (Balazs et al., 2014).

We believe these bispecific antibodies are candidates for clinical development, particularly as PrEP agents against HIV-1 transmission. There is now no doubt that PrEP with daily oral antiretroviral drug(s) works in preventing virus infection in humans, but the overall efficacy is limited by subject non-adherence (Baeten et al., 2013). Therefore, the use of long-acting antiviral agents could improve PrEP efficacy. The clinical development of a long-acting formulation of cabotegravir (Andrews et al., 2014) is well underway. Our lead bispecific antibodies could become useful additions to the armamentarium for HIV-1 prevention.

## EXPERIMENTAL PROCEDURES

### Reagents

MPER peptide and TZM-bl cells were obtained through the NIH AIDS Research and Reference Reagent Program, Division of AIDS, NIAID, NIH. Plasmids encoding a derivative IgG1 version of iMab were kindly provided by TaiMed Biologics, Inc.

### Construction, Expression and Purification of HIV CrossMAbs and Variants

Bispecific HIV CrossMAbs utilizing the knob-into-hole and light chain crossover formats were constructed as previously reported (Schaefer et al., 2011). Antigen targeting sequences for each HIV CrossMAb pair were synthesized (GeneArt Gene Synthesis and Life Technologies) using sequence information from previous reports[3–5,21,46,47], and each synthetic region was cloned into the pVAX expression plasmid (Life Technologies). Antibody-encoding DNA plasmid sequences were transiently transfected into Expi 293 cells (Life Technologies) using a 1:1:1:1 ratio by mass of the heavy-chain and light-chain plasmids encoding iMab or P140 and the heavy-chain and light-chain plasmids encoding the indicated HIV envelope targeting mAb. After overnight transfection, cells were cultured in serum-free hybridoma medium (Thermo Fisher Scientific). Cell culture supernatants were collected at 5 days post-transfection and purified as previously reported, with the modification that antibodies were quantified and purity was assessed using a NanoDrop Lite Spectrophotometer (ThermoFisher Scientific) (Pace et al., 2013b). Variants of parental HIV CrossMAbs were created by chimeric cloning using overlapping PCR or by using the Quik-Change II Site-Directed Mutagenesis kit as per the manufacturer's instructions (Agilent Technologies).

### Surface Plasmon Resonance

Binding affinity analyses of HIV CrossMAb 3BNC117/iMab for its respective ligands (monomeric gp120 HXBc2 and soluble human CD4) were performed in separate experiments with a Biacore 3000 optical biosensor (GE Healthcare) as previously described (Mouquet et al., 2012b) with the following additional modifications. Soluble human CD4 (Progenics Pharmaceuticals, Inc.) or gp120 HXBc2 (Sino Biological, Inc.) was immobilized

to CM5 sensor chips and binding kinetics were analyzed by flowing various concentrations of 3BNC117/iMab over the chip and monitoring association, then monitoring dissociation of bound 3BNC117/iMab while the surface was washed with buffer for 10 minutes. To investigate the interaction of both soluble CD4 and gp120 with 3BNC117/iMab, soluble human CD4 was immobilized to CM5 sensor chips, 3BNC117/iMab (flow sample 1) was flowed over the chip, then gp120 HXBc2 (flow sample 2) was flowed over the chip-sCD4-3BNC117/iMab complex.

### Pseudovirus Preparation and In Vitro Neutralization Assays

Pseudoviruses were prepared as previously described (Sun et al., 2014). Virus neutralization was assessed with a single cycle assay using TZM-bl cells and HIV-1 pseudoviruses as described previously (Seaman et al., 2010).

### Size Exclusion Chromatography

Size exclusion chromatography (SEC) was used to assess physicochemical homogeneity and to resolve monomers from non-monomeric species. Antibodies (20 ug) were analyzed using an AKTA purifier FPLC (GE Healthcare) with column, flow rate and mobile phase previously described (Pace et al., 2013b).

### Animal Studies

**Animal Ethics Statement—**All animals were bred and maintained at the Comparative Bioscience Center of The Rockefeller University in accordance with the regulations of its Institutional Animal Committee Care and Use Committee (IACUC). All animal studies were conducted under protocols approved by this committee.

**Antibody Evaluation in Wild-Type Mice—**BALB/c mice were divided into groups of three, and mice in each group were administered intraperitoneally with 100 μg of the indicated antibody. Blood was drawn from all animals at days 1, 2, 4, and 7 post antibody administration and serum was isolated and analyzed for levels of antibody in individual mice. For those animals in which antibody was detected at day 7, an additional blood collection at day 10 was performed and analyzed for antibody levels in serum. CoStar 96-Well EIA/RIA plates (Corning) were coated with 100 ng per well of goat anti-human IgG Fc-γ fragment (Jackson ImmunoResearch) overnight at 4°C. Plates were washed three times with PBS + Tween and blocked with PBS containing 5% milk and 0.5% BSA for 2 hours at room temperature. Mouse serum from the treated animals, and purified antibody in PBS for the standard curves, were added to the wells in 1:2 serial dilutions in PBS containing 2% milk and 0.2% BSA and incubated for 2 hours. After washing, peroxidase-conjugated goat anti-human IgG (Jackson ImmunoResearch) was incubated for 1 hour at room temperature. Samples were detected by TMB Liquid Substrate System (Sigma) and spectrophotometric readings were performed at 450 nm.

**Generation of Humanized Mice—**Generation of humanized mice was conducted as previously reported (Klein et al., 2012) with modifications. NSG (NOD.Cg-*Prkdc*$^{scid}$ *Il2rg*$^{tm1Wjl}$/SzJ) mice were obtained from The Jackson Laboratory. Newborn mice between day 1 and 5 were irradiated with 100 rads and then injected intrahepatically with $0.2\times10_6$

human hematopoietic $CD34^+$ stem cells 6 hours later. The level of human engraftment was assessed 8 weeks after transplantation. Mice with ≥ 65% $huCD45^+$ cells of total $CD45^+$ cells in peripheral blood were used for the studies; the average level of engraftment was 80.7 % for our experimental mice.

**HIV-1 Treatment and Prevention Studies in Humanized Mice—**$HIV\text{-}1_{JR\text{-}CSF}$ was produced in Expi 293 cells and collected 5 days after transfection, and 50% tissue culture infectious dose ($TCID_{50}$) was determined in TZM-bl cells and calculated by the Reed and Muench method (Reed and Muench, 1938). For the treatment experiment, mice were infected intraperitoneally at a dose of 250,000 $TCID_{50}$ per animal, which corresponded to a 100% animal infectious dose. For the prevention experiment, mice receiving $10E8_{V2.0}$/iMab were challenged by intraperitoneal injection at 200,000 $TCID_{50}$ one day after the first antibody administration and 4 weeks after the first antibody administration, and 250,000 $TCID_{50}$ 6 weeks after the first antibody administration. The animals were considered infected when two consecutive viral load measurements were above the limit of detection.

**Detection of HIV CrossMAb $10E8_{V2.0}$/iMab in Plasma from Humanized Mice—**CoStar 96-Well EIA/RIA plates (Corning) were coated with 20 ng sCD4 protein per well overnight at 4°C. Plates were washed three times with PBS + Tween and blocked with PBS containing 5% milk and 0.5% BSA for 2 hours at room temperature. Mouse plasma was inactivated by incubating in 1% Triton X-100 (Sigma) at room temperature for 5 minutes. Inactivated plasma was then added in 1:3 serial dilutions in PBS containing 2% milk and 0.2% BSA and incubated for 2 hours. Triton-inactivated $10E8_{V2.0}$/iMab was used in duplicate for the standard curve. After washing, peroxidase-conjugated goat anti-human IgG (Jackson ImmunoResearch) was incubated for 1 hour at room temperature. Samples were detected by TMB Liquid Substrate System (Sigma) and spectrophotometric readings were performed at 450 nm.

**Receptor Occupancy Assay—**50 μL of blood was collected retro-orbitally in EDTA-tubes from mice having received an i.p. administration of $10E8_{V2.0}$/iMab. The blood of each mouse was then divided into two conditions. The first was spiked with 0.5 μg of $10E8_{V2.0}$/iMab for 30 min at room temperature (RT) for the 100% receptor occupancy (RO) control, while the second was left untouched. All samples were then washed two times with PBS + 1% FBS and then stained with anti-human CD45 Pacific Orange, anti-human CD3 FITC, anti-human CD4 PerCP (ThermoFisher Scientific) and biotin anti-human Ig lambda light chain (BioLegend) for 30 minutes at room temperature. After one washing step, streptavidin PE (BioLegend) was added for 20 minutes, followed by 1X Lysing Buffer (BD Biosciences) for 20 min. Cells were then pelleted and resuspended in 1X CytoFix Buffer (BD Biosciences). The RO percentage was calculated as 100 * (Mean Fluorescence Intensity (MFI) of sample PE signal / MFI of spiked sample PE signal).

**Quantitative Reverse Transcription PCR Assay—**Plasma HIV-1 RNA was quantified every week as previously reported (Klein et al., 2012) with modifications. RNA was extracted from 100 μL of plasma using the Qiagen MinElute Virus Spin Kit (Qiagen) and eluted in 55 μL. The RT-PCR was performed in one step in 30 μL reaction containing 10 μL

of RNA, 1X TaqMan PCR mix, 1X TaqMan RT-enzyme mix (TaqMan RNA-to-Ct 1-Step Kit, Life Technologies), 500 mM of primers targeting a conserved region of Pol and 140 nM of probe. Cycling conditions were 15 min at 48°C, 17 min at 94°C, followed by 50 cycles at 95°C for 30 seconds and 60°C for 60 seconds. Samples were run in duplicate in a 7500 Fast Real-Time PCR System (Applied Biosystems) and the limit of detection was 200 copies/mL plasma.

**HIV-1 Envelope Sequence Analysis—**cDNA was generated following the SuperScript™ III Reverse Transcriptase (Thermo Fisher Scientific) manufacturer's instructions using the primer sequence 5'-TTGCTACTTGTGATTGCTCCATGT-3'. The *env* sequence was amplified by PCR using 0.5 U of HiFi Taq Polymerase and 200 nM of primers (5'-TAGAGCCCTGGAAGCATCCAGGAAG-3' and 5'-TTGCTACTTGTGATTGCTCCATGT-3'). The cycling conditions were 2 minutes at 94°C, followed by 35 cycles at 94°C for 15 seconds, 58°C for 30 seconds and 68°C for 4 minutes, followed by 10 minutes at 68°C. The product was used for nested PCR using 0.5 U of HiFi Taq Polymerase and 200 nM of primers (5'-TTAGGCATCTCCTATGGCAGGAAGAAG-3' and 5'-GTCTCGAGATACTGCTCCCACCC-3'). The same cycling conditions were used for 45 cycles. PCR products were sequenced by Genewiz, Inc. using a set of eight primers designed to cover the whole *env* sequence, and the sequences were analyzed and assembled using Geneious software (version 7.1.4) and aligned to JR-CSF sequence (GenBank: U45960.1). The mutations were numbered according to the HXB2 sequence using the Los Alamos Sequence Locator tool.

### Calculations and Statistical Analyses

$IC_{50}$ and maximum percent inhibition summary values across the panel of 118 Tier-2 HIV-1 Env pseudoviruses in Figure 1B indicate median ± interquartile ranges, and differences between pairs were calculated by student's t-test. Differences in viral load decreases between treated and PBS groups of humanized mice in Figure 5B were assessed by Mann-Whitney test. Statistical significance was achieved at $P \leq 0.05$. For the prevention study in Figure 6A, statistics were calculated by log-rank test. For the in vivo pharmacokinetic study in Figure 6B, data points represent the mean $10E8_{V2.0}$/iMab plasma concentrations from seven mice at each time point indicated, and the error bars represent the standard deviation. The mean $IC_{50}$ value for any particular antibody against the 118 multi-clade or 200 clade C pseudovirus panel presented throughout the text represents the geometric mean of the $IC_{50}$ values of that particular antibody against each pseudovirus in its respective panel. Fold increase or decrease in potencies for any set of antibodies presented throughout the text was calculated using the geometric mean $IC_{50}$ values of the antibody set against the pseudovirus panel stated.

## Supplementary Material

Refer to Web version on PubMed Central for supplementary material.

## Acknowledgments

We thank Faye Yu, Mar Boente-Carrera and Natanya Gettie for technical assistance; Brian T. Chait and Paul Dominic B. Olinares for native mass spectroscopy analyses on 10E8 and 10E8/P140; Wendy Chen for assistance with figure preparation; Michel Nussenzweig for providing neutralization data for 3BNC117; Mark Louder and John Mascola for providing neutralization data for the combination of 3BNC117, PG9, 10-1074 and 10E8; and members of the Ho laboratory for helpful discussions. D.D.H. was supported by the Bill and Melinda Gates Foundation's Collaboration for AIDS Vaccine Discovery (Grants OPP50714 and OPP1040732) and by the National Institutes of Health (Grant DP1DA033263). M.S.S. was supported by the Bill and Melinda Gates Foundation's Comprehensive Ab Vaccine Immune Monitoring Consortium (Grant 1032144). Competing financial interests statement: D.D.H. is the scientific founder of TaiMed Biologics, Inc., which owns the commercial rights to ibalizumab. In this capacity, D.D.H. has equity in the company. Y.H., J.Y. and D.D.H. are holders of a patent describing HIV CrossMAbs, including 10E8/iMab and 10E8/P140 and their variants, for HIV-1 prevention and therapy.

## REFERENCES

Andrews CD, Spreen WR, Mohri H, Moss L, Ford S, Gettie A, Russell-Lodrigue K, Bohm RP, Cheng-Mayer C, Hong Z, et al. Long-acting integrase inhibitor protects macaques from intrarectal simian/human immunodeficiency virus. Science. 2014; 343:1151–1154. [PubMed: 24594934]

Baeten JM, Haberer JE, Liu AY, Sista N. Preexposure prophylaxis for HIV prevention: where have we been and where are we going? J Acquir Immune Defic Syndr. 2013; 63(Suppl 2):S122–S129. [PubMed: 23764623]

Balazs AB, Chen J, Hong CM, Rao DS, Yang L, Baltimore D. Antibody-based protection against HIV infection by vectored immunoprophylaxis. Nature. 2012; 481:81–84. [PubMed: 22139420]

Balazs AB, Ouyang Y, Hong CM, Chen J, Nguyen SM, Rao DS, An DS, Baltimore D. Vectored immunoprophylaxis protects humanized mice from mucosal HIV transmission. Nature medicine. 2014; 20:296–300.

Barouch DH, Whitney JB, Moldt B, Klein F, Oliveira TY, Liu J, Stephenson KE, Chang HW, Shekhar K, Gupta S, et al. Therapeutic efficacy of potent neutralizing HIV-1-specific monoclonal antibodies in SHIV-infected rhesus monkeys. Nature. 2013; 503:224–228. [PubMed: 24172905]

Berges BK, Rowan MR. The utility of the new generation of humanized mice to study HIV-1 infection: transmission, prevention, pathogenesis, and treatment. Retrovirology. 2011; 8:65. [PubMed: 21835012]

Blattner C, Lee JH, Sliepen K, Derking R, Falkowska E, de la Pena AT, Cupo A, Julien JP, van Gils M, Lee PS, et al. Structural delineation of a quaternary, cleavage-dependent epitope at the gp41–gp120 interface on intact HIV-1 Env trimers. Immunity. 2014; 40:669–680. [PubMed: 24768348]

Burkly LC, Olson D, Shapiro R, Winkler G, Rosa JJ, Thomas DW, Williams C, Chisholm P. Inhibition of HIV infection by a novel CD4 domain 2-specific monoclonal antibody. Dissecting the basis for its inhibitory effect on HIV-induced cell fusion. J Immunol. 1992; 149:1779–1787. [PubMed: 1380539]

Caskey M, Klein F, Lorenzi JC, Seaman MS, West AP Jr, Buckley N, Kremer G, Nogueira L, Braunschweig M, Scheid JF, et al. Viraemia suppressed in HIV-1-infected humans by broadly neutralizing antibody 3BNC117. Nature. 2015; 522:487–491. [PubMed: 25855300]

Diskin R, Scheid JF, Marcovecchio PM, West AP Jr, Klein F, Gao H, Gnanapragasam PN, Abadir A, Seaman MS, Nussenzweig MC, et al. Increasing the potency and breadth of an HIV antibody by using structure-based rational design. Science. 2011; 334:1289–1293. [PubMed: 22033520]

Doria-Rose NA, Schramm CA, Gorman J, Moore PL, Bhiman JN, DeKosky BJ, Ernandes MJ, Georgiev IS, Kim HJ, Pancera M, et al. Developmental pathway for potent V1V2-directed HIV-neutralizing antibodies. Nature. 2014; 509:55–62. [PubMed: 24590074]

Gardner MR, Kattenhorn LM, Kondur HR, von Schaewen M, Dorfman T, Chiang JJ, Haworth KG, Decker JM, Alpert MD, Bailey CC, et al. AAV-expressed eCD4-Ig provides durable protection from multiple SHIV challenges. Nature. 2015; 519:87–91. [PubMed: 25707797]

Georgiev IS, Rudicell RS, Saunders KO, Shi W, Kirys T, McKee K, O'Dell S, Chuang GY, Yang ZY, Ofek G, et al. Antibodies VRC01 and 10E8 neutralize HIV-1 with high breadth and potency even

with Ig-framework regions substantially reverted to germline. J Immunol. 2014; 192:1100–1106. [PubMed: 24391217]

Goetze AM, Schenauer MR, Flynn GC. Assessing monoclonal antibody product quality attribute criticality through clinical studies. mAbs. 2010; 2:500–507. [PubMed: 20671426]

Halper-Stromberg A, Lu CL, Klein F, Horwitz JA, Bournazos S, Nogueira L, Eisenreich TR, Liu C, Gazumyan A, Schaefer U, et al. Broadly neutralizing antibodies and viral inducers decrease rebound from HIV-1 latent reservoirs in humanized mice. Cell. 2014; 158:989–999. [PubMed: 25131989]

Haverick M, Mengisen S, Shameem M, Ambrogelly A. Separation of mAbs molecular variants by analytical hydrophobic interaction chromatography HPLC: overview and applications. mAbs. 2014; 6:852–858. [PubMed: 24751784]

Huang J, Ofek G, Laub L, Louder MK, Doria-Rose NA, Longo NS, Imamichi H, Bailer RT, Chakrabarti B, Sharma SK, et al. Broad and potent neutralization of HIV-1 by a gp41-specific human antibody. Nature. 2012; 491:406–412. [PubMed: 23151583]

Hutterer KM, Hong RW, Lull J, Zhao X, Wang T, Pei R, Le ME, Borisov O, Piper R, Liu YD, et al. Monoclonal antibody disulfide reduction during manufacturing: Untangling process effects from product effects. mAbs. 2013; 5:608–613. [PubMed: 23751615]

Jacobson JM, Kuritzkes DR, Godofsky E, DeJesus E, Larson JA, Weinheimer SP, Lewis ST. Safety, pharmacokinetics, and antiretroviral activity of multiple doses of ibalizumab (formerly TNX-355), an anti-CD4 monoclonal antibody, in human immunodeficiency virus type 1-infected adults. Antimicrobial agents and chemotherapy. 2009; 53:450–457. [PubMed: 19015347]

Klein F, Halper-Stromberg A, Horwitz JA, Gruell H, Scheid JF, Bournazos S, Mouquet H, Spatz LA, Diskin R, Abadir A, et al. HIV therapy by a combination of broadly neutralizing antibodies in humanized mice. Nature. 2012; 492:118–122. [PubMed: 23103874]

Kong R, Louder MK, Wagh K, Bailer RT, deCamp A, Greene K, Gao H, Taft JD, Gazumyan A, Liu C, et al. Improving neutralization potency and breadth by combining broadly reactive HIV-1 antibodies targeting major neutralization epitopes. Journal of virology. 2015; 89:2659–2671. [PubMed: 25520506]

Koterba KL, Borgschulte T, Laird MW. Thioredoxin 1 is responsible for antibody disulfide reduction in CHO cell culture. Journal of biotechnology. 2012; 157:261–267. [PubMed: 22138638]

Liu H, Gaza-Bulseco G, Faldu D, Chumsae C, Sun J. Heterogeneity of monoclonal antibodies. Journal of pharmaceutical sciences. 2008; 97:2426–2447. [PubMed: 17828757]

Lowe D, Dudgeon K, Rouet R, Schofield P, Jermutus L, Christ D. Aggregation, stability, and formulation of human antibody therapeutics. Advances in protein chemistry and structural biology. 2011; 84:41–61. [PubMed: 21846562]

Luo XM, Lei MY, Feidi RA, West AP Jr, Balazs AB, Bjorkman PJ, Yang L, Baltimore D. Dimeric 2G12 as a potent protection against HIV-1. PLoS pathogens. 2010; 6:e1001225. [PubMed: 21187894]

Lynch RM, Boritz E, Coates EE, DeZure A, Madden P, Costner P, Enama ME, Plummer S, Holman L, Hendel CS, et al. Virologic effects of broadly neutralizing antibody VRC01 administration during chronic HIV-1 infection. Science translational medicine. 2015; 7:319ra206.

Mascola JR, Haynes BF. HIV-1 neutralizing antibodies: understanding nature's pathways. Immunological reviews. 2013; 254:225–244. [PubMed: 23772623]

Mouquet H, Scharf L, Euler Z, Liu Y, Eden C, Scheid JF, Halper-Stromberg A, Gnanapragasam PN, Spencer DI, Seaman MS, et al. Complex-type N-glycan recognition by potent broadly neutralizing HIV antibodies. Proceedings of the National Academy of Sciences of the United States of America. 2012a; 109:E3268–E3277. [PubMed: 23115339]

Mouquet H, Scheid JF, Zoller MJ, Krogsgaard M, Ott RG, Shukair S, Artyomov MN, Pietzsch J, Connors M, Pereyra F, et al. Polyreactivity increases the apparent affinity of anti-HIV antibodies by heteroligation. Nature. 2010; 467:591–595. [PubMed: 20882016]

Mouquet H, Warncke M, Scheid JF, Seaman MS, Nussenzweig MC. Enhanced HIV-1 neutralization by antibody heteroligation. Proceedings of the National Academy of Sciences of the United States of America. 2012b; 109:875–880. [PubMed: 22219363]

Mullan B, Dravis B, Lim A, Clarke A, Janes S, Lambooy P, Olson D, O'Riordan T, Ricart B, Tulloch AG. Disulphide bond reduction of a therapeutic monoclonal antibody during cell culture manufacturing operations. BMC proceedings. 2011; 5(Suppl 8):110.

Pace CS, Fordyce MW, Franco D, Kao CY, Seaman MS, Ho DD. Anti-CD4 monoclonal antibody ibalizumab exhibits breadth and potency against HIV-1, with natural resistance mediated by the loss of a V5 glycan in envelope. J Acquir Immune Defic Syndr. 2013a; 62:1–9. [PubMed: 23023102]

Pace CS, Song R, Ochsenbauer C, Andrews CD, Franco D, Yu J, Oren DA, Seaman MS, Ho DD. Bispecific antibodies directed to CD4 domain 2 and HIV envelope exhibit exceptional breadth and picomolar potency against HIV-1. Proceedings of the National Academy of Sciences of the United States of America. 2013b; 110:13540–13545. [PubMed: 23878231]

Reed LJ, Muench H. A simple method of estimating fifty percent endpoints. The American Journal of Hygiene. 1938; 27:493–497.

Reimann KA, Lin W, Bixler S, Browning B, Ehrenfels BN, Lucci J, Miatkowski K, Olson D, Parish TH, Rosa MD, et al. A humanized form of a CD4-specific monoclonal antibody exhibits decreased antigenicity and prolonged plasma half-life in rhesus monkeys while retaining its unique biological and antiviral properties. AIDS research and human retroviruses. 1997; 13:933–943. [PubMed: 9223409]

Rosati S, Yang Y, Barendregt A, Heck AJ. Detailed mass analysis of structural heterogeneity in monoclonal antibodies using native mass spectrometry. Nature protocols. 2014; 9:967–976. [PubMed: 24675736]

Rudicell RS, Kwon YD, Ko SY, Pegu A, Louder MK, Georgiev IS, Wu X, Zhu J, Boyington JC, Chen X, et al. Enhanced potency of a broadly neutralizing HIV-1 antibody in vitro improves protection against lentiviral infection in vivo. Journal of virology. 2014; 88:12669–12682. [PubMed: 25142607]

Salinas BA, Sathish HA, Shah AU, Carpenter JF, Randolph TW. Buffer-dependent fragmentation of a humanized full-length monoclonal antibody. Journal of pharmaceutical sciences. 2010; 99:2962–2974. [PubMed: 20091831]

Schaefer W, Regula JT, Bahner M, Schanzer J, Croasdale R, Durr H, Gassner C, Georges G, Kettenberger H, Imhof-Jung S, et al. Immunoglobulin domain crossover as a generic approach for the production of bispecific IgG antibodies. Proceedings of the National Academy of Sciences of the United States of America. 2011; 108:11187–11192. [PubMed: 21690412]

Scheid JF, Mouquet H, Ueberheide B, Diskin R, Klein F, Oliveira TY, Pietzsch J, Fenyo D, Abadir A, Velinzon K, et al. Sequence and structural convergence of broad and potent HIV antibodies that mimic CD4 binding. Science. 2011; 333:1633–1637. [PubMed: 21764753]

Seaman MS, Janes H, Hawkins N, Grandpre LE, Devoy C, Giri A, Coffey RT, Harris L, Wood B, Daniels MG, et al. Tiered categorization of a diverse panel of HIV-1 Env pseudoviruses for assessment of neutralizing antibodies. Journal of virology. 2010; 84:1439–1452. [PubMed: 19939925]

Sok D, van Gils MJ, Pauthner M, Julien JP, Saye-Francisco KL, Hsueh J, Briney B, Lee JH, Le KM, Lee PS, et al. Recombinant HIV envelope trimer selects for quaternary-dependent antibodies targeting the trimer apex. Proceedings of the National Academy of Sciences of the United States of America. 2014; 111:17624–17629. [PubMed: 25422458]

Song R, Franco D, Kao CY, Yu F, Huang Y, Ho DD. Epitope mapping of ibalizumab, a humanized anti-CD4 monoclonal antibody with anti-HIV-1 activity in infected patients. Journal of virology. 2010; 84:6935–6942. [PubMed: 20463063]

Stiegler G, Kunert R, Purtscher M, Wolbank S, Voglauer R, Steindl F, Katinger H. A potent cross-clade neutralizing human monoclonal antibody against a novel epitope on gp41 of human immunodeficiency virus type 1. AIDS research and human retroviruses. 2001; 17:1757–1765. [PubMed: 11788027]

Sun M, Pace CS, Yao X, Yu F, Padte NN, Huang Y, Seaman MS, Li Q, Ho DD. Rational design and characterization of the novel, broad and potent bispecific HIV-1 neutralizing antibody iMabm36. J Acquir Immune Defic Syndr. 2014; 66:473–483. [PubMed: 24853313]

Tenorio AR. The monoclonal CCR5 antibody PRO-140: the promise of once-weekly HIV therapy. Current HIV/AIDS reports. 2011; 8:1–3. [PubMed: 21170687]

Toma J, Weinheimer SP, Stawiski E, Whitcomb JM, Lewis ST, Petropoulos CJ, Huang W. Loss of asparagine-linked glycosylation sites in variable region 5 of human immunodeficiency virus type 1 envelope is associated with resistance to CD4 antibody ibalizumab. Journal of virology. 2011; 85:3872–3880. [PubMed: 21289125]

Trkola A, Ketas TJ, Nagashima KA, Zhao L, Cilliers T, Morris L, Moore JP, Maddon PJ, Olson WC. Potent, broad-spectrum inhibition of human immunodeficiency virus type 1 by the CCR5 monoclonal antibody PRO 140. Journal of virology. 2001; 75:579–588. [PubMed: 11134270]

Walker LM, Huber M, Doores KJ, Falkowska E, Pejchal R, Julien JP, Wang SK, Ramos A, Chan-Hui PY, Moyle M, et al. Broad neutralization coverage of HIV by multiple highly potent antibodies. Nature. 2011; 477:466–470. [PubMed: 21849977]

Walker LM, Phogat SK, Chan-Hui PY, Wagner D, Phung P, Goss JL, Wrin T, Simek MD, Fling S, Mitcham JL, et al. Broad and potent neutralizing antibodies from an African donor reveal a new HIV-1 vaccine target. Science. 2009; 326:285–289. [PubMed: 19729618]

Wu X, Yang ZY, Li Y, Hogerkorp CM, Schief WR, Seaman MS, Zhou T, Schmidt SD, Wu L, Xu L, et al. Rational design of envelope identifies broadly neutralizing human monoclonal antibodies to HIV-1. Science. 2010; 329:856–861. [PubMed: 20616233]

Zhu J, Ofek G, Yang Y, Zhang B, Louder MK, Lu G, McKee K, Pancera M, Skinner J, Zhang Z, et al. Mining the antibodyome for HIV-1-neutralizing antibodies with next-generation sequencing and phylogenetic pairing of heavy/light chains. Proceedings of the National Academy of Sciences of the United States of America. 2013; 110:6470–6475. [PubMed: 23536288]

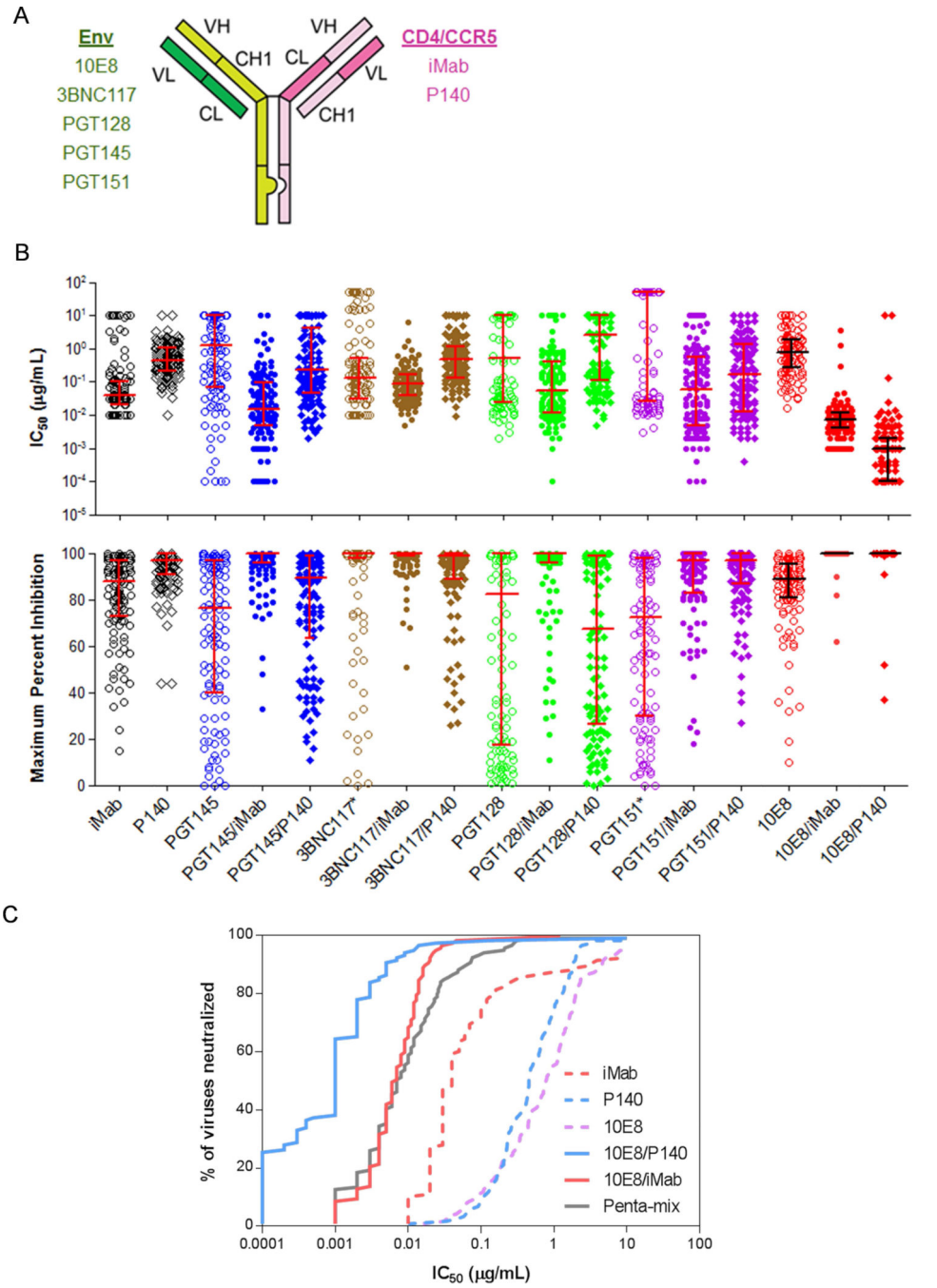


**Figure 1. HIV CrossMAbs possess potent and broad antiviral activity against a diverse panel of 118 Tier-2 HIV-1 Env pseudoviruses**

**(A)** Schematic of an HIV CrossMAb and list of examples of parental antibodies from which each CrossMAb was derived. **(B)** $IC_{50}$ (top panel) and maximum percent inhibition (MPI, bottom panel) comparison of select HIV CrossMAbs and their parental mAbs. Asterisks refer to data obtained from other sources (3BNC117 MPI data from personal communication with Michel Nussenzweig and PGT151 $IC_{50}$ and MPI data from Blattner et al., 2014). Error bars indicate median ± interquartile range. **(C)** Percent of viruses neutralized (based on $IC_{50}$

values) by 10E8/P140 and 10E8/iMab, and their parental mAbs. Neutralization by penta-mix is included as a reference (Klein et al., 2012).

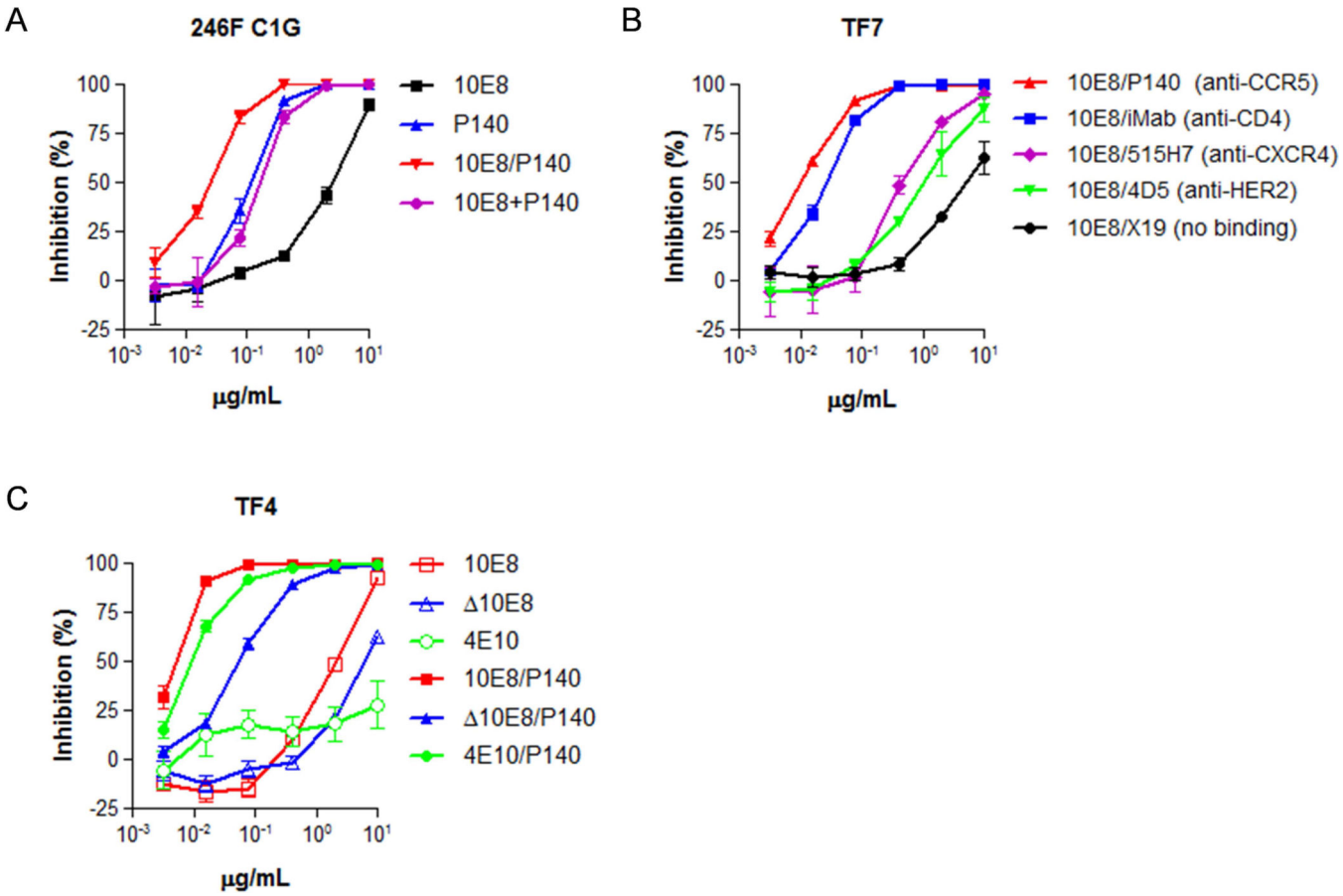


**Figure 2. Neutralization studies to elucidate the mechanism of action of a potent HIV CrossMAb**

**(A)** Neutralization of the representative HIV-1 pseudovirus 246F C1G by 10E8/P140, parental mAbs individually, or parental mAbs in combination. **(B)** Neutralization of the representative pseudovirus TF7 by bispecific antibodies comprised of a 10E8 antibody moiety and one of several host cell receptor targeting antibody moieties. **(C)** Neutralization of the representative HIV-1 pseudovirus TF4 by MPER-binding mAbs or CCR5-anchored MPER-binding bispecific antibodies.

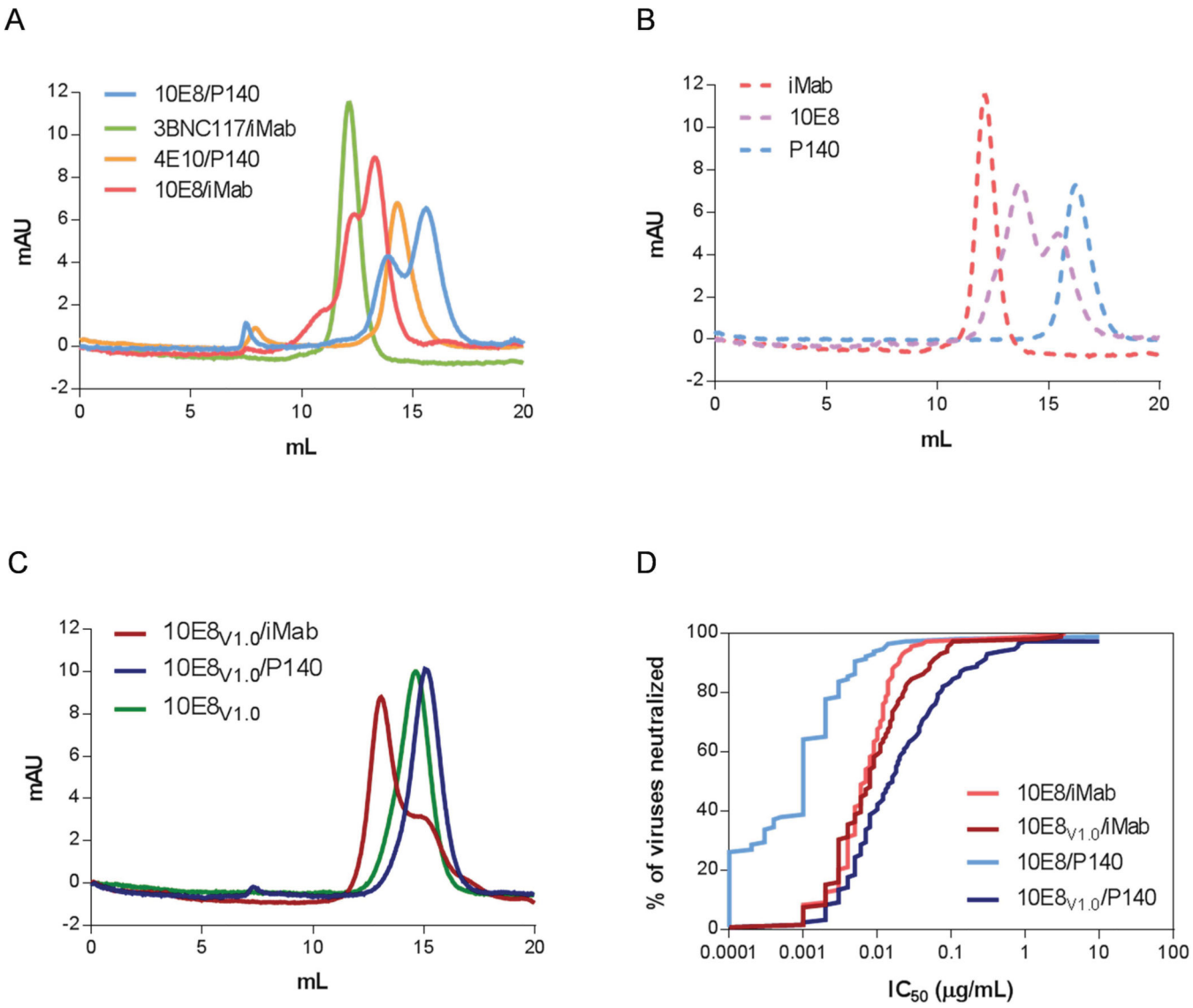


**Figure 3. 10E8 mAb and 10E8-containing CrossMAbs exhibit physicochemical heterogeneity**

**(A)** SEC analysis of 10E8/P140, 3BNC117/iMab, 4E10/P140 and 10E8/iMab. **(B)** SEC analysis of parental mAbs iMab, 10E8 and P140. **(C)** SEC analysis of $10E8_{V1.0}$/iMab and $10E8_{V1.0}$/P140 and mAb variant $10E8_{V1.0}$. **(D)** Percent of viruses of a 118 Tier-2 HIV-1 Env pseudovirus panel neutralized (based on $IC_{50}$ values) by 10E8/iMab and 10E8/P140 and engineered variants $10E8_{V1.0}$/iMab and $10E8_{V1.0}$/P140.

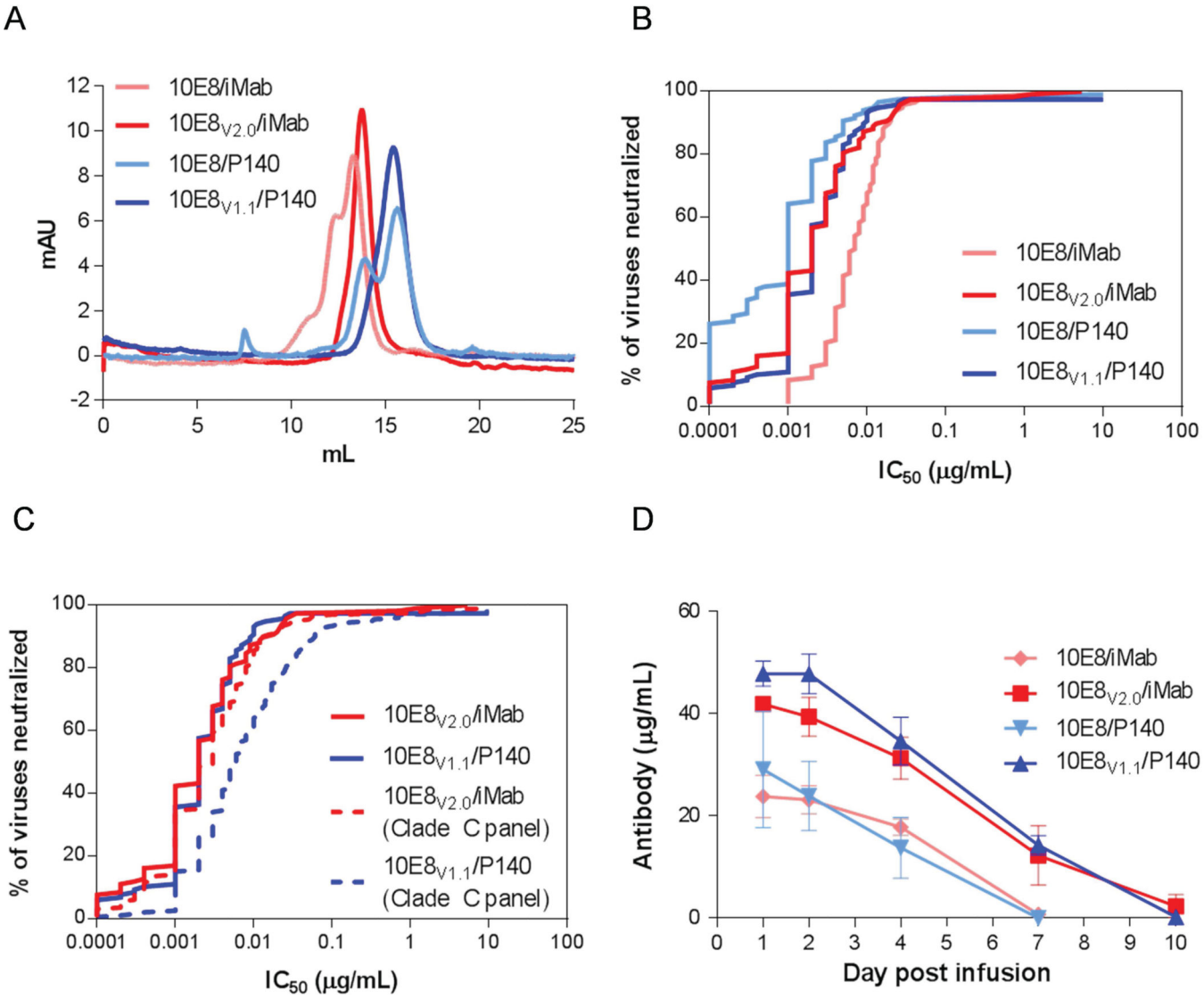


**Figure 4. Engineering HIV CrossMAb variants with improved developability, activity and manufacturability potential**

**(A)** SEC analysis and **(B)** percent of a 118 Tier-2 HIV-1 Env pseudovirus panel neutralized by the originally identified 10E8/iMab and 10E8/P140 and engineered variants $10E8_{V2.0}$/iMab and $10E8_{V1.1}$/P140. **(C)** Percent of a panel of 200 clade C Env pseudoviruses neutralized by $10E8_{V2.0}$/iMab and $10E8_{V1.1}$/P140. The neutralization profiles of these two candidates against the 118 virus panel from Figure 1D are overlaid for ease of comparison. **(D)** Serum concentration of the indicated HIV CrossMAb after 100 μg intraperitoneal administration to mice. Error bars represent standard error of mean.

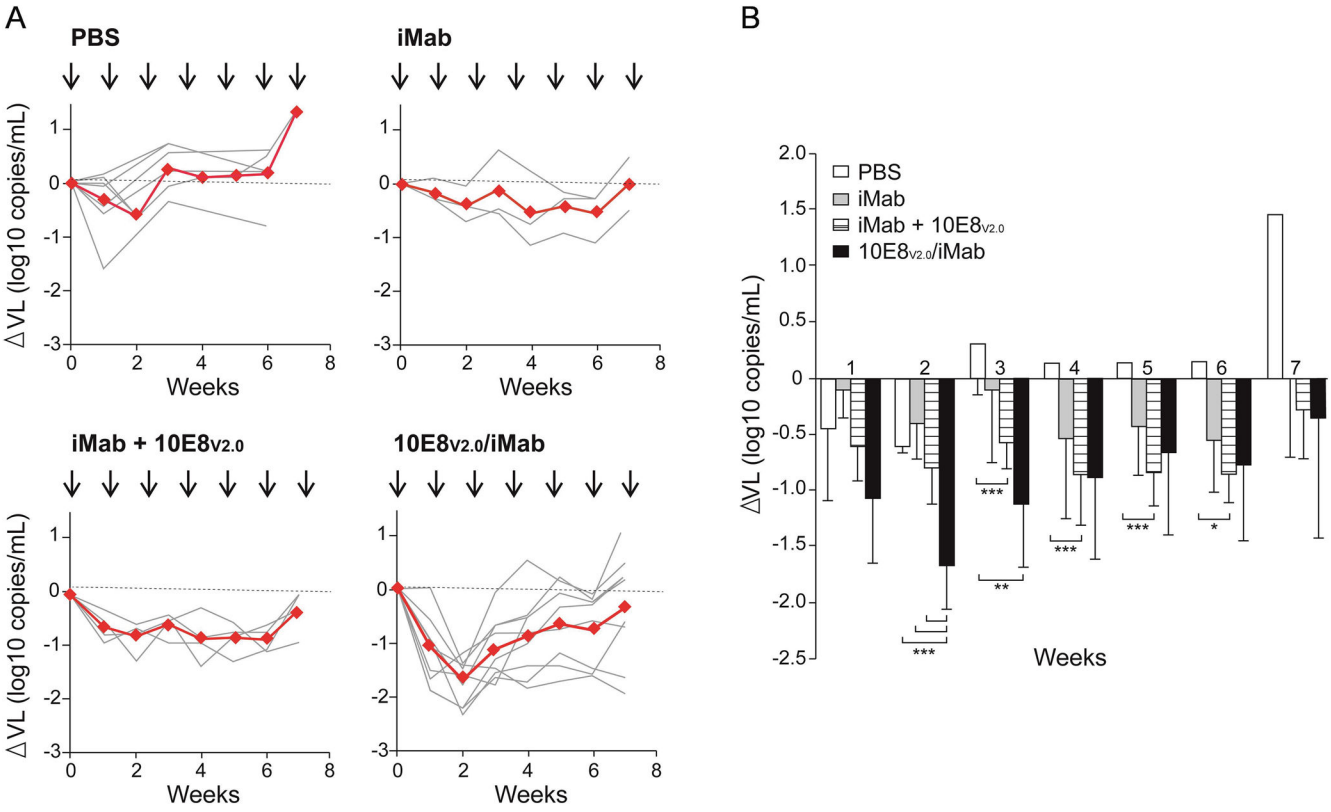


C

| | iMab associated resistance | | 10E8$_{V2.0}$ associated resistance |
|---|---|---|---|
| | C3 region (335-344) | V5 region (458-467) | MPER region (671-683) |
| JR-CSF WT | RAQWNNTLKQ | GGKNESEIEI | NWFDITKWLWYIK |
| PBS | | | |
| iMab | T.I<br>D<br>D | G | |
| iMab + 10E8$_{V2.0}$ | T<br>Y<br>D<br>D | R<br>I<br>N | P<br>P |
| 10E8$_{V2.0}$/iMab | D | N | L<br>L<br>G<br>L<br>L<br>P |

D

| | iMab | 10E8 | 10E8$_{V2.0}$/iMab |
|---|---|---|---|
| WT | 0.043 | 0.063 | 0.002 |
| G410R | 0.073 | 0.093 | 0.003 |
| N339D | 4.306 | 0.263 | 0.013 |
| S463N | >50 | 0.143 | 0.013 |
| W672G | 0.143 | 2.034 | 0.563 |
| W672L | 0.113 | 0.413 | 0.353 |
| F673L | 0.113 | 0.173 | 0.273 |

**Figure 5. HIV CrossMAb 10E8$_{V2.0}$/iMab exhibits therapeutic efficacy in vivo**

**(A)** Changes in plasma viral RNA from baseline at week 0. Grey lines represent data from each mouse, whereas the red lines represent the mean for each group. NSG humanized mice were infected with JR-CSF at week −4 and the antibody treatment consisting of weekly 500 μg antibody injections (arrows) began at week 0. **(B)** Comparison of the therapeutic efficacy of 10E8$_{V2.0}$/iMab with the comparator groups. Columns represent changes in viral load. * $p < 0.05$, ** $p < 0.01$, *** $p < 0.001$ as determined by the Mann-Whitney test. **(C)** Mutations in HIV-1 Env associated with resistance after viral rebound. Colored amino acids and dashes

indicate the positions of mutations and deletions, respectively. All mutations are aligned to the JR-CSF sequence and numbered according to the HXB2 sequence. **(D)** $IC_{50}$ concentrations (μg/mL) of the antibodies listed in the top row against wild-type HIV-$1_{JR-CSF}$ or mutants containing the indicated mutations in the HIV-$1_{JR-CSF}$ envelope shown in the left column. Red indicates $IC_{50}$ < 0.2 μg/mL, orange indicates $IC_{50}$ between 0.2 and 2 μg/mL, yellow indicates $IC_{50}$ between 2 and 20 μg/mL and white indicates $IC_{50}$ > 20 μg/mL.

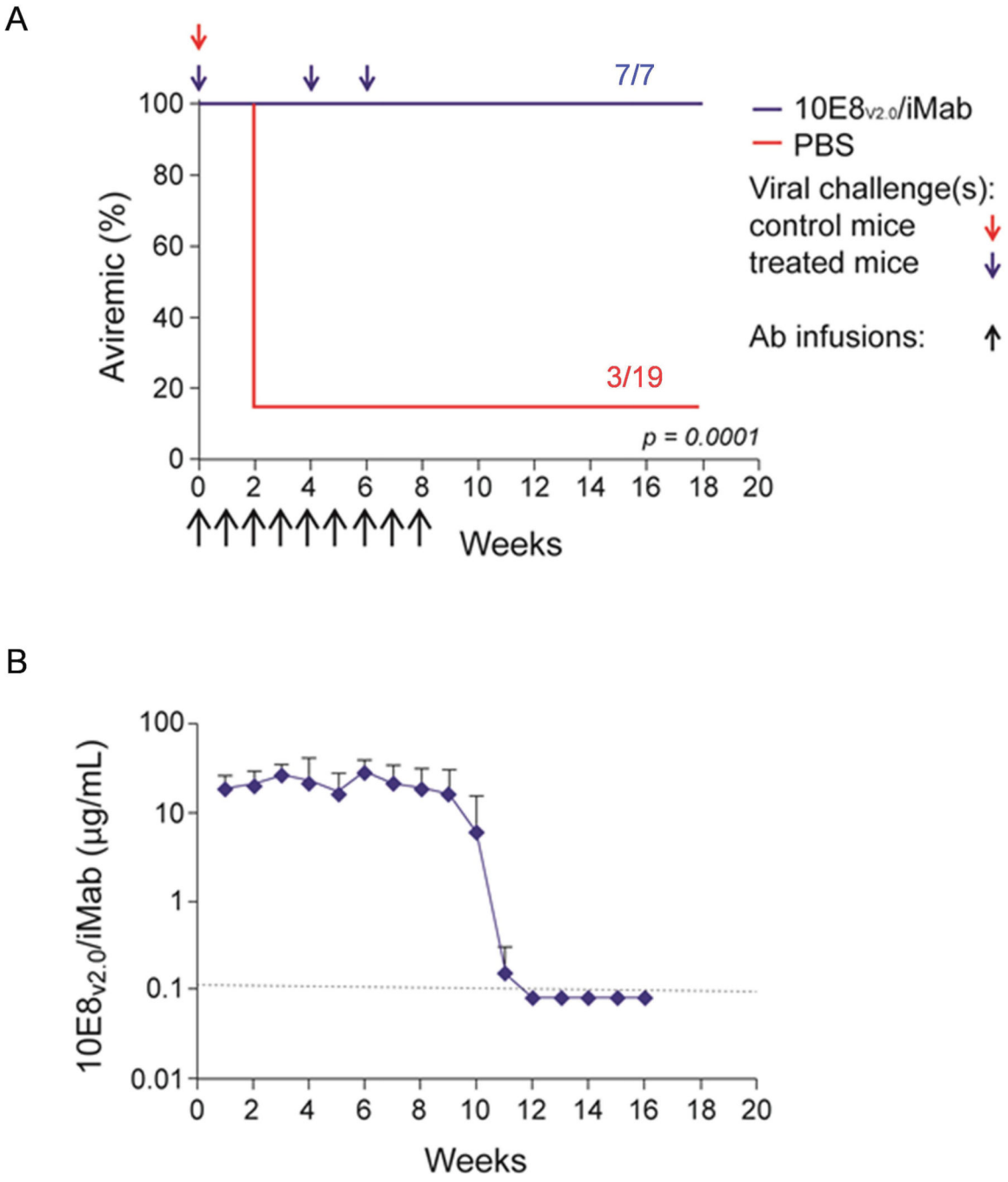


**Figure 6. HIV CrossMAb 10E8$_{V2.0}$/iMab protects humanized mice against repeated systemic HIV-1 challenges**

**(A)** Kaplan-Meier plot depicting the percentage of aviremic mice in 10E8$_{V2.0}$/iMab-treated versus PBS-treated challenged mice. Mice received 200 µg of 10E8$_{V2.0}$/iMab every week from week 0 to week 8 (black arrows) and were challenged at day 1 and weeks 4 and 6 (blue arrows). PBS control mice were challenged once at day 1 (red arrow). Statistics were calculated by log-rank test. **(B)** Quantification of 10E8$_{V2.0}$/iMab plasma concentration by ELISA. The dashed line represents the limit of detection at 0.11 µg/mL. Values below the

limit of detection are arbitrarily plotted at 0.09 μg/mL. Error bars represent the standard deviation.

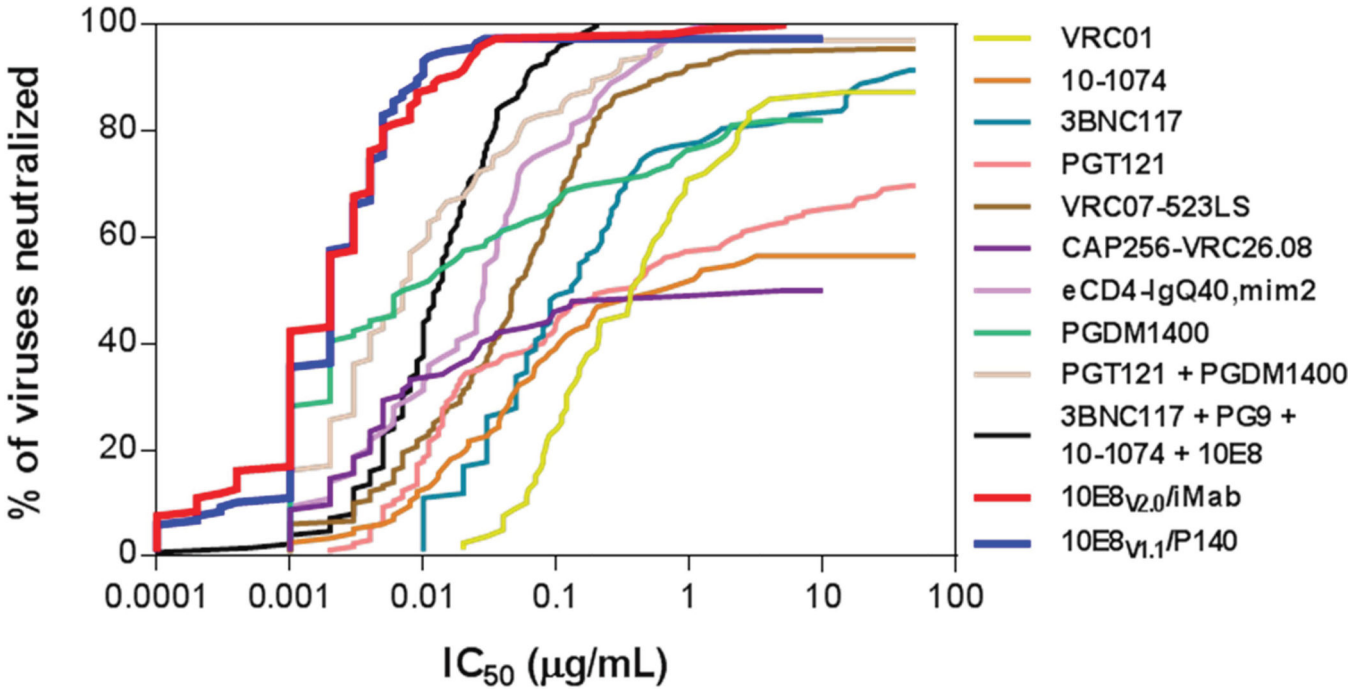


**Figure 7. Percent of large panels of multi-clade HIV-1 Env pseudoviruses neutralized by antibodies currently in development for HIV-1 prevention**

Antiviral coverage of $10E8_{V2.0}$/iMab and $10E8_{V1.1}$/P140 are reported in this manuscript; antiviral coverage of all other molecules presented are from previously published data (Gardner et al., 2015; Kong et al., 2015; Mouquet et al., 2012a; Rudicell et al., 2014; Scheid et al., 2011; Sok et al., 2014; Wu et al., 2010).